Extended Abstracts of the 2006 International Conference on Solid State Devices and Materials, Yokohama, 2006, pp. 848-849

B-8-1

40G bit/s NRZ wavelength converter with narrow active waveguides and inverted operation

Tatsuo Hatta[1,2,3], Toshiharu Miyahara[1,2], Yasunori Miyazaki[1,2], Kazuhisa Takagi[1,2],
Keisuke Matsumoto[1,2], Toshitaka Aoyagi[1,2], Ken Mishina[3], Akihiro Maruta[3], and Kenichi Kitayama[3]

[1]Optoelectronic Industry and Technology Development Association (OITDA),
4-1,Mizuhara, Itami, Hyogo, 664-8641, Japan
Phone: +81-72-780-2653 Fax:+81-72-780-3774 E-mail: Hatta.Tatsuo@bx.MitsubishiElectric.co.jp
[2]Mitsubishi Electric Corporation, 4-1, Mizuhara, Itami, Hyogo, 664-8641, Japan
[3]Osaka University, Department of Electrical, Electronics and Information Engineering, Graduate School Engineering,
2-1, Yamadaoka, Suita, Osaka, 565-0871, Japan

1. Introduction

As demand for higher communication bandwidth continues to grow, current optical-electronic-optical (O-E-O) conversion-based routers face considerable challenges to scale to large capacities due to power consumption, space and cost restrictions. All-optical solution such as optical burst switching is a strong candidate for next generation communication infrastructure [1].

Wavelength converter is one of the key active devices which solve wavelength contention in all-optical burst switching network [2]. In order to apply wavelength converter to the practical metropolitan area where communication *traffic jam* is most critical, we need to establish the connectivity with existing optical transceivers.

Mask of the eye diagram is a good indicator of connectivity, so that we apply the mask specified in ITU-T G.693 to the output waveform of wavelength converter. Monolithically integrated chip parameter is optimized to cope with existing network specifications up to 40Gbit/s.

2. Device structure

Figure 1 shows the schematic of the monolithically integrated wavelength converter. Semiconductor optical amplifier (SOA) is located on each arm and connected by transparent passive waveguide and multi-mode interference (MMI) coupler. The band-gap of the transparent waveguide is 1.3 µm. Gain peak wavelength of SOA is 1.55 µm.

Fig. 2 shows the top view of the monolithic wavelength converter chip. The SOAs were butt-jointed with passive waveguides to form a Mach-Zehnder interferometer (MZI). The chip size was 4,800µm x 720µm. In order to reduce the optical reflection and suppress SOA lasing even under high gain operating conditions, the interface between the SOA and the passive waveguide has a 45º-tilted butt-joint [3], and the facet reflectivity was reduced by an anti-reflection coating and a window structure.

Figure 3 shows the photograph of wavelength converter module and its optics. Wavelength converter chip is mounted on hermetically-sealed thermo-electric cooler and kept its temperature to 25ºC. Input-port waveguides are fabricated with 25µm intervals, and optically couple with 125µm fiber array by aspherical lens. Attained coupling efficiencies are higher than 50%.

Fig. 1 Schematic of the wavelength converter chip.

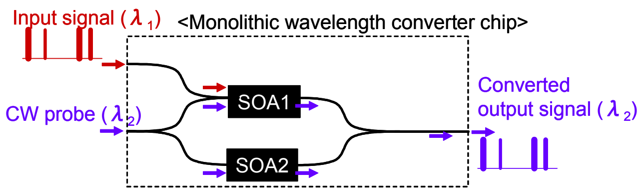

Fig. 2 Top view of the monolithic chip.

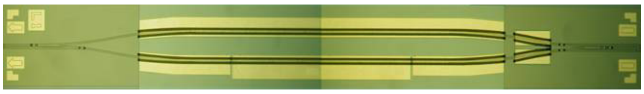

Fig. 3 Wavelength converter module and its optics.

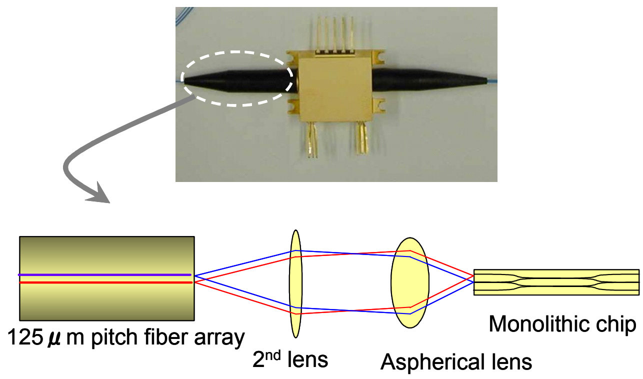

2. Narrow waveguide design

SOA width and length are optimized in order to get the maximum eye-opening after wavelength conversion. Theoretical calculations are based on the rate equation model to assess the effect of longitudinal variations in electron and photon densities in the SOA on the wavelength conversion process [4]. Figure 4 shows the calculated waveform for each waveguide width. The narrower the waveguide width, the larger the eye-opening becomes, because SOA current effectively increase the carrier density. 0.6-µm width, which is far below the standard size for semiconductor lasers, is narrow enough to operate at 40G bit/s. In order to achieve the high carrier density, we have improved the blocking layer fabrication process.

Fig. 5 shows the calculated waveform for each waveguide length. At the length of 1.8mm, strong pattern effect is observed, whereas, sufficient eye openings are observed at the length greater than 2.4mm.

According to the above mentioned calculation results, the size of SOA waveguides are decided to 0.6μm wide and 2.4mm long.

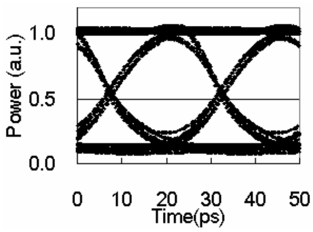

(a) w=0.6μm

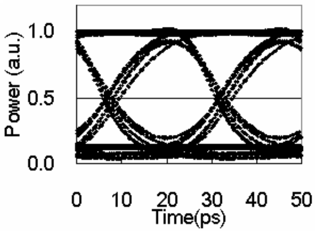

(b) w=1.0μm

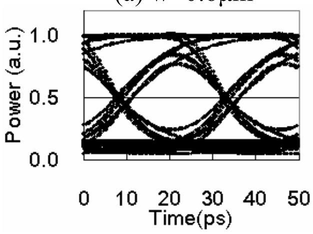

(c) w=1.4μm

Fig. 4 Simulated waveform for each waveguide width.

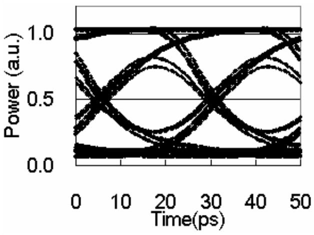

(a) L=1.8mm

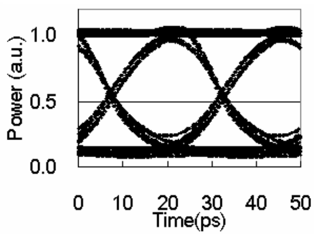

(b) L=2.4mm

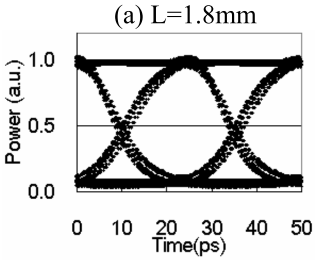

(c) L=3.0mm

Fig. 5 Simulated waveform for each SOA length.

3. Inverted vs. non-inverted operation

Figure 6 shows the calculated waveform for XGM and XPM operation. XGM waveform shows the 3dB extinction ratio, which is reflected to the output power difference between inverted and non-inverted XPM operation. This clearly indicates that inverted operation is preferable from the optical SNR point of view in order for XGM to support the XPM operation.

Figure 7(a) shows the XGM waveform which is well consistent with the calculated one. Inverted XPM waveform complies with the ITU-T G.693 eye-mask as shown in Figure 7(b).

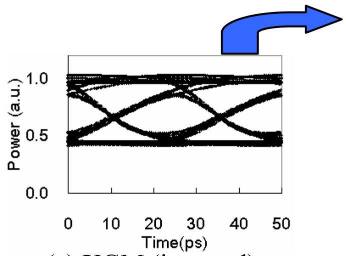

(a) XGM (inverted)

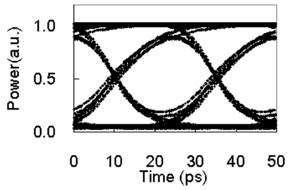

(b) XPM (inverted)

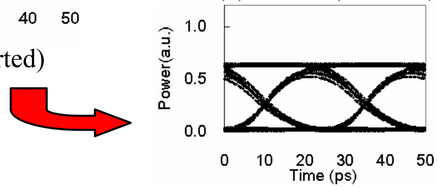

(c) XPM (non-inverted)

Fig. 6 Calculated waveform for XGM and XPM operation.

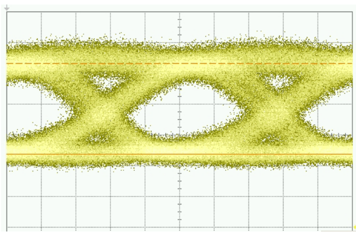

(a)XGM waveform (inverted, Ex.=3dB).

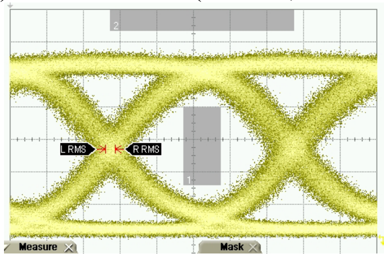

(b) XPM waveform (inverted, Ex.=10dB)

Fig. 7 Measured XGM and XPM waveform for 40G bit/s.

4. Conclusions

Performance of monolithically-integrated SOA-MZI wavelength converter was improved by narrow, 0.6μm-width active SOA waveguide. Eye-mask-compliant 40G bit/s NRZ waveform was successfully demonstrated with inverted operation.

Acknowledgements

This work was partially performed under the management of the Optoelectronic Industry and Technology Development Association (OITDA) supported by New Energy and Industrial Technology Development Organization (NEDO).

References

[1] K. Kitayama et al., J. Lightwave Technol., vol.23, No.10, Oct. 2005, pp3404-3418.

[2] A. Al Amin et al., OFC/NFOEC 2006 , OFO5.

[3] T. Miyahara et al., OECC2005, paper 8F1-1.

[4] M. Asghari et al., J. Lightwave Technol., vol.15, No.7, July 1997, pp1181-1190.